

# High Density and Super Ultra-Microporous-Activated Carbon Macrospheres with High Volumetric Capacity for CO<sub>2</sub> Capture


Jingjing Liu, Xin Liu, Yuan Sun, Chenggong Sun,\* Hao Liu,\* Lee A. Stevens, Kaixi Li, and Colin E. Snape

Activated carbon (AC) spheres with a diameter of 1.0–2.0 mm are synthesized from coal tar pitch for postcombustion carbon capture. The as-prepared AC macrospheres after potassium hydroxide (KOH) activation are found to possess extraordinarily developed microporosity of which 87% is ultra-microporosity with pore diameters less than 0.8 nm. Despite the relatively low surface area of just 714 m<sup>2</sup> g<sup>-1</sup> with a pore volume of 0.285 cm<sup>3</sup> g<sup>-1</sup>, the macrospherical carbon adsorbents achieve exceedingly high CO<sub>2</sub> uptake capacities of 3.15 and 1.86 mmol g<sup>-1</sup> at 0 and 25 °C, respectively, with a CO<sub>2</sub> partial pressure of 0.15 bar. Cyclic lifetime performance testing demonstrates that the CO<sub>2</sub> uptake is fully reversible with fast adsorption and desorption kinetics. More importantly, due to their high bulk density of ≈1.0 g cm<sup>-3</sup>, the AC macrospheres exhibit extremely high volumetric CO<sub>2</sub> uptakes of up to 81.8 g L<sup>-1</sup> at 25 °C at 0.15 bar CO<sub>2</sub>, which represents the highest value ever reported for ACs. The high ultra-microporosity coupled with the potassium-modified physiochemical surface properties is found to be responsible for the outstanding CO<sub>2</sub> adsorption performance of the pitch-based AC macrospheres.

## 1. Introduction

The rising concentration of CO<sub>2</sub> in the atmosphere due to excessive use of fossil fuels has caused increasing concerns as a result of its impact on global climate change.<sup>[1]</sup> There has been

Dr. J. Liu, Dr. X. Liu, Y. Sun, Dr. C. Sun, Prof. H. Liu, Dr. L. A. Stevens, Prof. C. E. Snape  
Faculty of Engineering  
The Energy Technologies Building  
Jubilee Campus  
University of Nottingham  
Nottingham NG7 2TU, UK  
E-mail: cheng-gong.sun@nottingham.ac.uk; liu.hao@nottingham.ac.uk  
Prof. K. Li  
Institute of Coal Chemistry  
Chinese Academy of Sciences  
Taiyuan, Shanxi 03001, China

 The ORCID identification number(s) for the author(s) of this article can be found under <https://doi.org/10.1002/adsu.201700115>.

© 2017 The Authors. Published by WILEY-VCH Verlag GmbH & Co. KGaA, Weinheim. This is an open access article under the terms of the Creative Commons Attribution License, which permits use, distribution and reproduction in any medium, provided the original work is properly cited.

DOI: 10.1002/adsu.201700115

a major research effort to develop novel materials and technologies for CO<sub>2</sub> capture that have lower energy penalties than the established first-generation technology of aqueous amine scrubbing.<sup>[2]</sup> As well as relatively high energy consumptions, there are corrosion and toxicity issues with amine scrubbing.<sup>[2a,3]</sup> Solid adsorbents have received great interests with carbon-based materials, metal–organic frameworks (MOFs), zeolites, alkali-metal bicarbonate/carbonate, and amine-functionalized/supported sorbents having been the focus of many investigations.<sup>[4]</sup>

Among all the promising adsorbents, activated carbon (AC) materials<sup>[5]</sup> have been considered as one of the materials with most potential, as a result of their low cost, high surface area, moderate heat of adsorption for CO<sub>2</sub>, good regeneration ability, and wide availability.<sup>[6]</sup>

As physical adsorbents, the CO<sub>2</sub> capture capacity of carbon-based materials is largely determined by their textural properties and surface chemistries. Due to the nature of physical adsorption, the main drawback of AC sorbents lies in their reduced CO<sub>2</sub> uptakes at high adsorption temperatures and low CO<sub>2</sub> partial pressures, which greatly restricts its application for postcombustion carbon capture under typical flue gas conditions. For example, at 0.15 bar CO<sub>2</sub>, the capacity of porous carbons decreased from 1.25 to 0.40 mmol g<sup>-1</sup> when temperature raised from 25 to 60 °C while the CO<sub>2</sub> uptake was reduced from 3.1 to 0.9 mmol g<sup>-1</sup> when the pressure decreased from 1 to 0.1 bar at 25 °C.<sup>[7]</sup> In order to improve the performance of AC for CO<sub>2</sub> capture under possible real flue gas conditions, a significant number of investigations have been carried out toward enhancing the surface area and tuning the pore structure/size via different activation methodologies, and surface modification via manipulating the precursor materials and/or pre-/postactivation treatments.<sup>[8]</sup> Among different approaches, two main methodologies have been agreed that can markedly increase CO<sub>2</sub> capture capacities at low partial pressures: design of ultra-micropores below 0.8 nm to enhance the micropore filling mechanism;<sup>[9]</sup> and surface modification via nitrogen doping,<sup>[10]</sup> to improve the affinity between AC adsorption sites and CO<sub>2</sub>. Thanks to all the past research efforts, the CO<sub>2</sub> uptake capacities at 25 °C and 0.15 bar

CO<sub>2</sub> for some porous carbon materials have been increased to 1.5–1.8 mmol g<sup>-1</sup>[6g,10d,11] on a weight basis.

However, as most of the reported adsorbent materials, if not all, usually have very low bulk densities due to their high porosity, they are expected to give rise to low CO<sub>2</sub> uptake capacities on a volumetric basis despite their high adsorption capacities on a weight basis. Nevertheless, the importance of achieving high adsorption capacities on a volumetric basis of an adsorbent material, which is critical in determining the ultimate energy and capture efficiency of a solid adsorbent-based capture system, has received little attention in the most previous investigations where increasing the porosity of AC carbons has been pursued as one of the major means to increase their CO<sub>2</sub> adsorptive properties. Clearly, given the limited volume of a capture system, it is essential to maximize both of the adsorption capacity and the density for the adsorbents under practical flue gas stream conditions.<sup>[12]</sup> In addition, most of the AC materials reported previously were produced in the power forms with particle sizes in the range of micrometers, which greatly restricts their direct practical applications on large scales with either fluidized-bed and/or moving bed operations while the further engineering of the materials for desirable shapes and particle sizes will lead to losses in CO<sub>2</sub> adsorption performance.<sup>[6d]</sup>

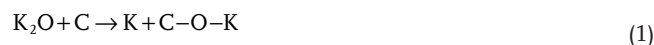
In this paper, we report a pitch-based AC macrospheres with diameters of 1.0–2.0 mm, which give the highest volumetric CO<sub>2</sub> uptake ever reported at low CO<sub>2</sub> partial pressure (0.15 bar at 25 °C). The one-step KOH activation was employed as a means to produce carbons with highly ultra-microporous structures with potassium intercalated in the structures. Gravimetric and volumetric CO<sub>2</sub> adsorption capacities, bulk density, mechanical strength, and regenerability of macrocarbon spheres were also investigated in this paper in the light of industrial applications.

## 2. Results and Discussion

### 2.1. Chemical Properties of Pitch-Based Spheres

The chemical compositions of pitch-based carbons were determined by elemental analysis and X-ray fluorescence (XRF), and the results are summarized in **Table 1**. The results indicate that after KOH treatment, the K and O contents increase remarkably as expected, while the amount of H and C decreases. On the other hand, the N and S contents remain consistent after KOH activation. The reaction mechanism of KOH and carbon is a well-established activation method

of producing porous AC materials. During the activation process, the reaction between the formed K<sub>2</sub>O and carbon can lead to the formation of functional groups such as C–O–K at high temperature of 700 °C as shown below.<sup>[13]</sup> The presence of –O–K in the char further results in the oxidation of crosslinking carbon atoms and then creates carbon surface rich in oxygen functional groups at the edges of the lamella, such as hydroxyl, carbonyl, carboxylic and carbonyl anhydride, and so on,<sup>[14]</sup> which gives rise to the usually high content of oxygen in the carbons from the chemical activation, as shown in **Table 1**. It is believed that the potassium produced in the activation, in situ, has been intercalated into the lamella of carbon matrix and after activation, they exist in their intercalated forms that associated with different oxygen functionalities, leading the formation of quasi-chemical species (C–O–K). In our previous investigations, we have investigated the formation of intercalated potassium species.<sup>[15a,b]</sup> According to our previous results of X-ray photoelectron spectroscopic characterizations, it was found that after KOH treatment, the K 2p spectrum for the potassium in the carbon samples exhibited two peaks at 293.2 and 296.0 eV, respectively, with an intensity ratio of 2:1 and a difference of 2.8 eV in binding energy, which is characteristic of the spin–orbit split doublet (K 2p<sub>3/2</sub> and K 2p<sub>1/2</sub>) of surface potassium cations and oxides.<sup>[15]</sup> This suggests that the formation of strongly bound potassium surface complexes presumably in the form of O<sup>δ-</sup>–K<sup>δ+</sup> or extra framework K<sup>+</sup> cations. It is believed that similar structures were also formed in the pitch-derived carbon beads from using the same activation protocol. The potassium-containing surface groups cannot be easily removed even with excessive water washing, which can be indicated by the remaining potassium, close to 6 wt% after washing with abundant deionized water.



### 2.2. Textural Properties of Pitch-Based Spheres

The N<sub>2</sub> adsorption isotherms are presented in **Figure 1a**. It can be clearly seen that the isotherms for both K-treated pitch samples display type I isotherms. Adsorption increases rapidly below relative pressure  $P/P_0$  of 0.1, and then reaches a plateau, revealing the typical microporous nature of the samples. Apparently, sample PAC1.0\_700 (where PAC refers to Pitch-based Activated Carbon) prepared from using a higher KOH/carbon ratio have a greater developed porosity than sample PAC0.5\_700 (**Table 1**). PAC1.0\_700 has a higher Brunauer–Emmett–Teller

**Table 1.** Texture properties and chemical compositions of pitch carbons.

Sample	Textural properties				Chemical compositions [wt%]					
	S <sub>BET</sub> [m <sup>2</sup> g <sup>-1</sup> ]	V <sub>total</sub> [cm <sup>3</sup> g <sup>-1</sup> ]	V <sub>micro</sub> <sup>a)</sup> [cm <sup>3</sup> g <sup>-1</sup> ]	V <sub>narrow</sub> <sup>b)</sup> [cm <sup>3</sup> g <sup>-1</sup> ]	C	N	H	S	K <sup>c)</sup>	O <sup>d)</sup>
PAC0	1	–	–	–	91.6	1.5	3.4	0.7	0.0	2.8
PAC0.5_700	714	0.285	0.280	0.244	83.9	1.1	0.8	0.6	6.3	7.3
PAC1.0_700	974	0.381	0.378	0.331	83.6	1.2	0.5	0.6	5.9	8.2

<sup>a)</sup>Pore volume of micropores (2 nm) was calculated by cumulative pore volume using NLDFT model; <sup>b)</sup>Pore volume of narrow micropores (<0.8 nm), which was calculated by cumulative pore volume using NLDFT model; <sup>c)</sup>The content of potassium was determined by XRF; <sup>d)</sup>The content of oxygen was obtained by difference.

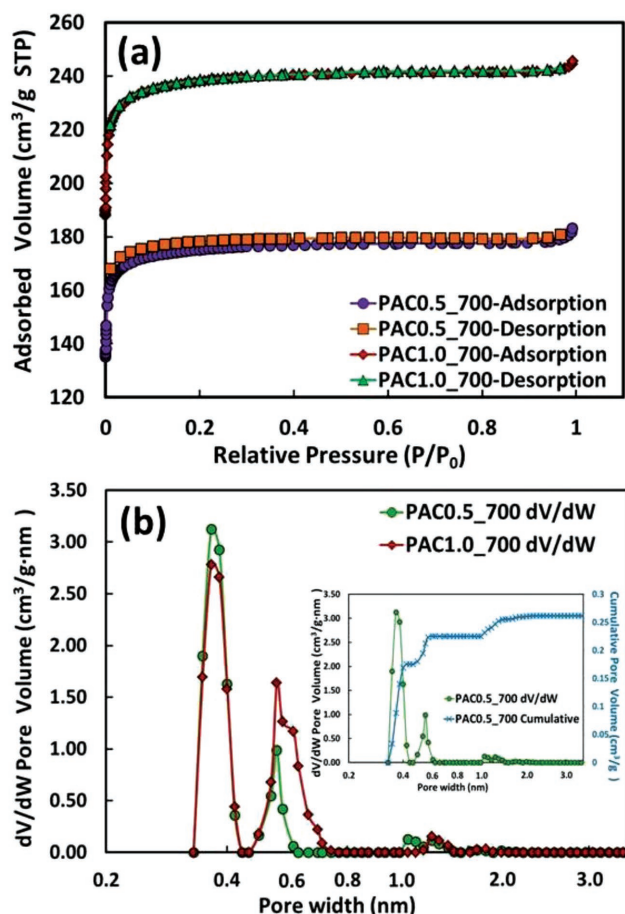


**Figure 1.** a)  $N_2$  isotherms at  $-196\text{ }^\circ\text{C}$  and b) pore size distributions for PAC0.5\_700 and PAC1.0\_700; the inner picture in (b) shows the relationship of  $dV/dW$  and cumulative pore volume against pore width for PAC0.5\_700.

(BET) specific surface area of  $974\text{ m}^2\text{ g}^{-1}$  and a higher total pore volume of  $0.381\text{ cm}^3\text{ g}^{-1}$  than PAC0.5\_700 ( $714\text{ m}^2\text{ g}^{-1}$  and  $0.285\text{ cm}^3\text{ g}^{-1}$ , respectively), which is clearly attributable to enhanced KOH activation.

Figure 1b shows the pore size distribution of K-treated pitch spheres. In general, the K-treated pitch carbons present well-developed microporosity, especially narrow micropores with sizes below  $0.8\text{ nm}$ . Basically, except for a small peak around  $1.1$  and  $1.2\text{ nm}$ , both prepared samples have shown a bimodal micropore distribution, i.e.,  $0.36$  and  $0.52\text{ nm}$  for PAC0.5\_700; and  $0.38$  and  $0.61\text{ nm}$  for PAC1.0\_700. With increasing KOH/carbon ratio, the peaks in the pore size distributions were slightly shifted to larger diameters, possibly resulting from the enlargement of the narrow micropores as a result of the enhanced activation. For instance, the inserted picture of Figure 1b illustrates both the  $dV/dW$  and cumulative pore volume against pore width for PAC0.5\_700. It was found that for PAC0.5\_700, the volume of micropores  $V_{\text{micro}}$  ( $<2\text{ nm}$ ) is  $0.280\text{ cm}^3\text{ g}^{-1}$ , which accounts for up to 98% of the total porosity, and more importantly, the volume of narrower or ultra-micropores  $V_{\text{narrow}}$  ( $<0.8\text{ nm}$ ) is  $0.244\text{ cm}^3\text{ g}^{-1}$ , which represents 87% of the total microporosity. Such extraordinary ultra-microporosity with rarely seen narrow pore size

distributions observed for these pitch-based macrospheres can usually only be obtained with MOFs prepared from using specific ligand precursors.<sup>[16]</sup> It has been previously reported that ultra-microporosity plays a vital role in determining the physical  $\text{CO}_2$  adsorption capacity of carbons particularly at low  $\text{CO}_2$  partial pressures.

Compared with other reported ACs with considerably larger surface areas (normally larger than  $2000\text{ m}^2\text{ g}^{-1}$  [13a,17]), one significant feature of the pitch macrospheres is its moderate surface area ( $<1000\text{ m}^2\text{ g}^{-1}$ ) and pore volumes, thanks to the mild KOH activation conditions used, which appears to be essential to give rise to the desirable ultra-microporous structure without sacrificing the bulk density and mechanical strength. Figure 2 shows the morphology of pitch beads before and after KOH activation. As shown in Figure 2b–d, it is evident that the cracks or tunnels become more severe with the increase of KOH/carbon mass ratio from 0.5:1 for PAC0.5\_700 to 1:1 for PAC1.0\_700. The enlarged close-up view of PAC1.0\_700 illustrated in Figure 2d reveals that the initial worm-like tunnels have supplied a prior platform for KOH to react with the pitch matrix at activation temperatures as to form numerous micropores. It means that the prepared samples have hierarchical macro-micropore structure. The existence of interconnecting macropores or tunnels could be beneficial for  $\text{CO}_2$  to facilitate diffusion into the micropores.

### 2.3. $\text{CO}_2$ Adsorption Performance

#### 2.3.1. Static Adsorption Measurement

The  $\text{CO}_2$  adsorption isotherms of PAC0.5\_700 and PAC1.0\_700 at  $0$  and  $25\text{ }^\circ\text{C}$  up to  $1\text{ bar}$  are depicted in Figure 3. The corresponding  $\text{CO}_2$  uptakes at  $0.15$  and  $1\text{ bar}$  of  $\text{CO}_2$  are listed in Table 2. Owing to the reduced kinetic energy of  $\text{CO}_2$  gas molecules at lower temperature, the samples have shown higher  $\text{CO}_2$  uptakes at  $0\text{ }^\circ\text{C}$  than that at  $25\text{ }^\circ\text{C}$ . At the same given activation temperature ( $700\text{ }^\circ\text{C}$ ), the  $\text{CO}_2$  uptakes of two samples are mainly determined by the amount of used activation agent. However, it is apparent that at  $25\text{ }^\circ\text{C}$ , the  $\text{CO}_2$  adsorption isotherms for the two samples did not show any obvious difference. For instance, at  $25\text{ }^\circ\text{C}$  and  $0.15\text{ bar}$ , PAC0.5\_700 presents a  $\text{CO}_2$  uptake of  $1.86\text{ mmol g}^{-1}$ , compared with  $1.83\text{ mmol g}^{-1}$  for PAC1.0\_700. Similarly, at  $25\text{ }^\circ\text{C}$  and  $1.0\text{ bar}$ , the  $\text{CO}_2$  uptakes for PAC0.5\_700 and PAC1.0\_700 are increased to  $3.95$  and  $4.03\text{ mmol g}^{-1}$ , respectively. On the other hand, at  $0\text{ }^\circ\text{C}$ , the  $\text{CO}_2$  adsorption uptakes of PAC0.5\_700 are slightly higher than PAC1.0\_700 in the beginning, then the  $\text{CO}_2$  uptakes of PAC1.0\_700 greatly exceed that of PAC0.5\_700 from  $\approx 0.2\text{ bar}$  onward. This phenomenon can be attributed to the fact that at relatively low  $\text{CO}_2$  partial pressure such as  $0.15\text{ bar}$ , the smaller micropores are preferred for adsorption of  $\text{CO}_2$  molecules due to their stronger adsorption potential.

Table 2 shows a comparison between the pitch spheres and other N-doped porous carbons at  $0$  and  $25\text{ }^\circ\text{C}$  under atmospheric pressure as well as a  $\text{CO}_2$  partial pressure of  $0.15\text{ bar}$  which is a typical quantity for postcombustion flue gas. Given the fact that the pitch spheres have very low N contents, it is outstanding that the pitch samples have shown competitive  $\text{CO}_2$  uptakes compared with other carbons, especially at



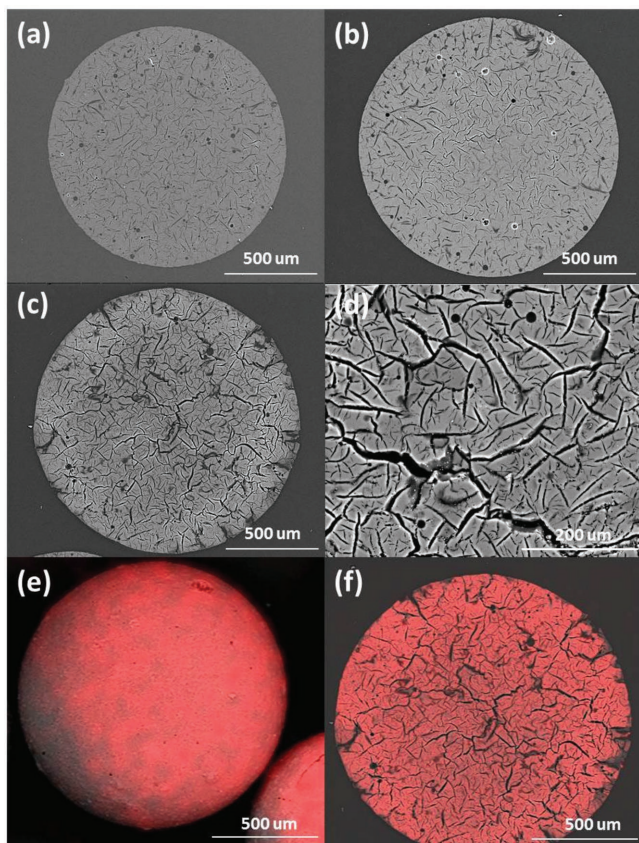


**Figure 2.** SEM images of a) original pitch sphere PAC0, b) PAC0.5\_700 with KOH/carbon mass ratio of 0.5:1, c) PAC1.0\_700 with KOH/carbon mass ratio of 1:1, and d) close up view of PAC1.0\_700; EDX elemental mapping of K of e) one carbon bead and f) cross-section of sample PAC1.0\_700.

0.15 bar. It can be seen from Table 2 that the pitch-derived macrospheres have achieved a CO<sub>2</sub> capacity of up to 3.15 and 1.86 mmol g<sup>-1</sup>, respectively, at 0 and 25 °C and 0.15 bar CO<sub>2</sub>,

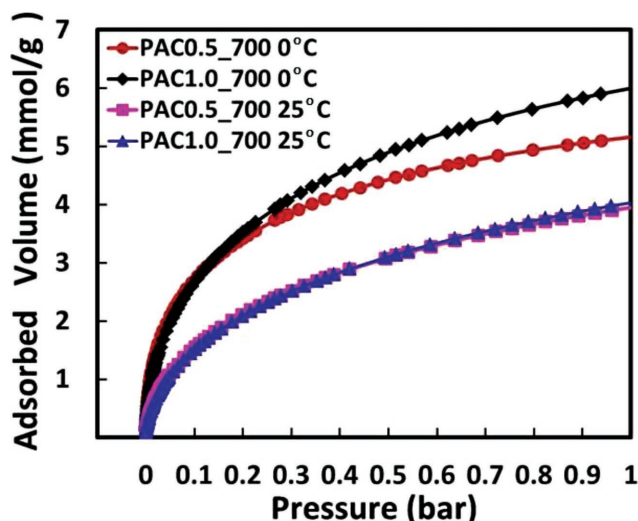


**Figure 3.** CO<sub>2</sub> adsorption isotherms of PAC0.5\_700 and PAC1.0\_700 at 0 and 25 °C from 0 to 1 bar.

**Table 2.** Comparison of CO<sub>2</sub> adsorption capacities with other N-doped AC adsorbents.

Sample	CO <sub>2</sub> capacity at 0 °C [mmol g <sup>-1</sup> ]		CO <sub>2</sub> capacity at 25 °C [mmol g <sup>-1</sup> ]		Ref.
	0.15 bar <sup>a)</sup>	1 bar	0.15 bar <sup>a)</sup>	1 bar	
CP-2-600	2.10	6.20	1.08	3.90	[10e]
CEM750	1.70	6.92	0.98	4.38	[23]
CSA-700	2.38	5.75	1.64	3.80	[10d]
SA-2N-P	3.15	8.99	1.51	4.57	[29]
NAC-1.5-600	2.95	7.2	1.70	5.38	[24]
PAC0.5_700	3.13	5.16	1.86	3.95	This work
PAC1.0_700	3.15	6.00	1.83	4.03	This work

All results are measured by static volumetric method; <sup>a)</sup>CO<sub>2</sub> uptakes at 0.15 bar were measured from the graph; CP-2-600: Polypyrrole based, CEM750: Acetonitrile-based template from zeolite, CSA-700: Polyacrylonitrile based, SA-2N-P: Sodium alginate based, NAC-1.5-600: Polyvinylidene fluoride based.

which is comparable or even better than those of other best-performing N-enriched carbon materials ranging from 1.70 to 3.15 mmol g<sup>-1</sup> and 0.98 to 1.7 mmol g<sup>-1</sup> under the similar adsorption conditions. It is worthy noted, however, that the CO<sub>2</sub> capacities for other N-containing carbons were obtained in their fine powder forms, which can be subjected to significant losses in adsorption capacity when they are transformed to larger particle sizes for practical applications. One significant explanation of the enhanced CO<sub>2</sub> uptakes at low CO<sub>2</sub> pressure is ascribed to the well-developed microporous structure, especially narrow micropores. Presser et al. claimed that at 0 °C under 1 bar, the micropores smaller than 0.8 nm would contribute to the majority of CO<sub>2</sub> uptakes on N-free carbide-derived carbons and at 0.1 bar, pore smaller or equal to 0.5 nm were preferred.<sup>[18]</sup> Zhang et al. further investigated the critical pore sizes that played a crucial role in CO<sub>2</sub> adsorption at different temperatures, i.e., the critical pore size (0.80, 0.70, and 0.54 nm for 0, 25, and 75 °C, respectively) decreased with the increase of adsorption temperature.<sup>[19]</sup>

However, based on the fact that the synthesized pitch spheres have lower surface area than the most reported carbons (normally more than 1000 m<sup>2</sup> g<sup>-1</sup><sup>[20]</sup>), the texture properties alone cannot account for the extraordinary large CO<sub>2</sub> uptakes. As for N-free samples, it is reasonable to believe that the excess CO<sub>2</sub> uptakes are associated with the extra framework of K cations formed from potassium intercalation during the KOH activation process in the carbon lattice. The distribution of potassium in carbon was carried out by elemental mapping for PAC1.0\_700, as illustrated in Figure 2e,f, where the intensity of red color represents the concentration of potassium. It is clearly shown that potassium is uniformly dispersed within the entire carbon framework. In our previous work,<sup>[15a]</sup> we have observed that due to potassium intercalation, the CO<sub>2</sub> capacity for phenolic resin carbons markedly increased from 0.79 to 1.51 mmol g<sup>-1</sup> at 25 °C and a CO<sub>2</sub> partial pressure of 0.15 bar. Similar to the efficacy of extra framework in zeolites and MOFs,<sup>[21]</sup> the formation of surface C–O–K group can enhance the electrostatic field so as to polarize adsorbate molecules to the surface.<sup>[22]</sup> According to our results, the influence of K doping on CO<sub>2</sub>

uptakes is quite comparable to, if not better than, that of nitrogen enrichment for carbon materials, particularly at low CO<sub>2</sub> partial pressures. Hence, K-doping pitch-based spheres with highly narrow microporous structures have been shown to be a great potential for postcombustion carbon capture processes.

### 2.3.2. Dynamic Adsorption Measurement and Cyclic Testing of Pitch-Based Spheres

The dynamic adsorption characteristics of PAC samples from thermogravimetric analyzer (TGA) at 25 °C and 0.15 bar CO<sub>2</sub> in balanced N<sub>2</sub> have been depicted in Figure 4a. As shown in Figure 4a, the CO<sub>2</sub> uptakes for PAC0.5\_700 and PAC1.0\_700 can achieve 89% and 92% of the equilibrium capacities within 5 min, which are 1.60 and 1.71 mmol g<sup>-1</sup>, respectively, compared with 1.80 and 1.85 mmol g<sup>-1</sup> as the equilibrium capacities after 60 min. The results are quite consistent with those obtained from static BET volumetric measurements. The observations also highlight the fast CO<sub>2</sub> adsorption kinetics for both pitch samples. It is believed that the hierarchical structure in pitch beads provides a desirable diffusion system for CO<sub>2</sub> adsorption, i.e., the macroporous interconnecting tunnels can be considered as expressway for CO<sub>2</sub> molecules to reach the micropores.

Figure 4b demonstrates the cyclic adsorption/desorption testing results for PAC samples. In general, both samples illustrate stable and excellent adsorption capacities over a long lifetime. More specifically, both PAC0.5\_700 and PAC1.0\_700 can maintain more than 90% of CO<sub>2</sub> uptake after 50 cycles by temperature swing. The slight early decrease for PAC1.0\_700 may be due to the irreversible CO<sub>2</sub> adsorption on K-containing compounds, typically including KOH and K<sub>2</sub>CO<sub>3</sub> that survived the excessive water washing and were loosely distributed onto the surfaces. The high CO<sub>2</sub> capacity and good regenerability of the dense carbon macrospheres in simulated flue gas stream proves their sound promise for postcombustion CO<sub>2</sub> capture applications.

### 2.3.3. Volumetric CO<sub>2</sub> Capacities

It is well known that for carbon-based adsorbents, the textural properties play an important role in determining their gravimetric CO<sub>2</sub> capacities. However, good textural properties with increased porosity are always accompanied by accordingly reduced bulk density, which can limit the amount of materials by mass that can be used for the given volume of a capture unit. This can potentially give rise to great reductions in

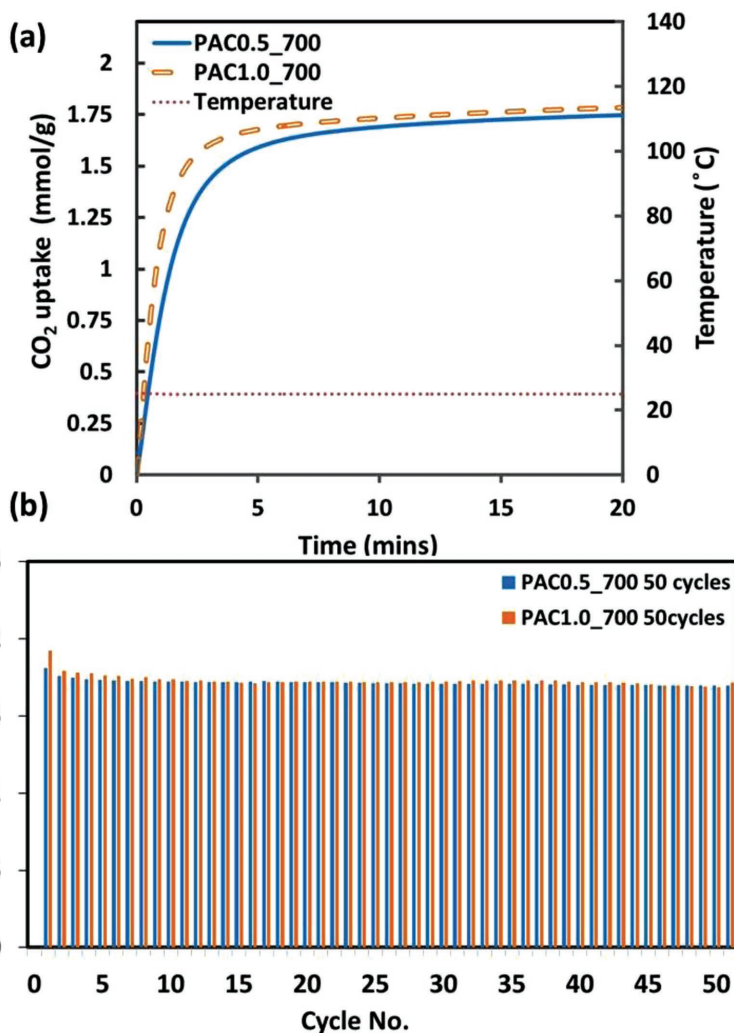


**Figure 4.** The CO<sub>2</sub> adsorption of PAC0.5\_700 and PAC1.0\_700 in a CO<sub>2</sub> partial pressure of 0.15 bar balanced by N<sub>2</sub> gas flow at 25 °C in a) single cycle of adsorption and b) 50 cycles of adsorption and desorption.

capture capacity under practical application conditions if on a weight basis, the gain in adsorption capacity from increased porosity does not sufficiently compensate for the loss in the capacity on a volumetric basis.<sup>[25]</sup> The volumetric adsorption capacity of an adsorbent material is not only determined by its gravimetric adsorption capacity but also by its density, which is usually low for highly ACs and high for less ACs.<sup>[12c]</sup> Table 3 compares the bulk densities of different carbon adsorbents produced from using different precursors, with silica supported Polyethylenimine (PEI) as a benchmark, which has been tested with superior performance in fluidized bed reactor.<sup>[26]</sup> The bulk density of raw pitch beads (PRO) before activation is found to possess the highest value of 1.14 g cm<sup>-3</sup>. Despite the slight decrease in density observed with the increase of KOH/carbon mass ratios, the bulk densities of the AC macrosphere samples, which vary from 1.00 g cm<sup>-3</sup> for the sample PAC0.5\_700 to 0.76 g cm<sup>-3</sup> for PAC1.0\_700, are still significantly higher than those of other materials reported. It is noteworthy that the PAC0.5\_700 carbon beads present even higher density than

**Table 3.** Comparison of bulk density of pitch spheres and other adsorbents.

Sample	Description	Form	Bulk density [g cm <sup>-3</sup> ]
PEI/silica <sup>a)</sup>	40% PEI loading	Powder (100–250 μm)	0.60
R2030 <sup>b)</sup>	Norit carbon purchased from Sigma Aldrich	Powder (200–325 μm)	0.52
MPPY2600 <sup>c)</sup>	Polypyrrole	Pressed discal pellets (≈1.3 cm)	0.85
PR3_700 <sup>d)</sup>	Phenolic Resin	Spheres (0.6–0.8 mm)	0.39
PAC0	Raw coal tar pitch	–	1.14 (1.23) <sup>e)</sup>
PAC0.5_700	Coal tar pitch	Spheres (1.0–2.0 mm)	1.00 (1.09) <sup>e)</sup>
PAC1.0_700	Coal tar pitch	–	0.76 (0.82) <sup>e)</sup>

<sup>a)</sup>Data from reference<sup>[26]</sup>; <sup>b)</sup>Data from reference<sup>[28]</sup>; <sup>c)</sup>Data from reference<sup>[27]</sup>; <sup>d)</sup>Data from reference<sup>[15a]</sup>; <sup>e)</sup>Denotes tap density.

MPPY2600 that was prepared by mechanical compression of polypyrrole-derived AC.<sup>[27]</sup> The measurements of the tap densities of pitch-based bead samples were also performed, and it was found that despite being slightly higher, the tap densities of the carbon beads were overall comparable to the bulk densities measured by Mercury Intrusion Porosimeter (MIP). The results are in line with the measurements of BET surface areas and scanning electron microscope (SEM) images.

The gravimetric and volumetric CO<sub>2</sub> uptakes for the adsorbents shown in Table 3 are also plotted in Figure 5 for better comparison. It can be observed that coupled with their exceedingly high CO<sub>2</sub> uptake capacities, the significantly higher densities of the pitch-based AC macrospheres have enabled them to achieve the highest CO<sub>2</sub> capacities on a volumetric basis among all other materials reported, including both the benchmark silica-PEI and the pressed MPPY2600 pellets despite their higher gravimetric CO<sub>2</sub> capacities. For instance, the CO<sub>2</sub> uptake of MPPY2600, PR3\_700, and silica-PEI at 25 °C and 0.15 bar CO<sub>2</sub> is 92.4, 79.2, and 101.2 mg g<sup>-1</sup>, compared with 81.8 mg g<sup>-1</sup>

for PAC0.5\_700 and 80.5 mg g<sup>-1</sup> for PAC1.0\_700. However, on a more useful volumetric basis, the PAC0.5\_700 pitch macrospheres achieved a remarkable capacity of 81.8 g L<sup>-1</sup>, being considerably higher than those of silica-PEI (60.7 g L<sup>-1</sup>), MPPY2600 (78.5 g L<sup>-1</sup>), and PR3\_700 (30.9 g L<sup>-1</sup>). Please note that the volumetric capacity of the pitch-based carbons was measured on a macroscale of 1.0–2.0 mm, hence the value for other reported materials (except for MPPY2600) may be overestimated because they were measured for their fine power forms, and the making of larger particles from fine powders via palletization or sphericalization always leads to significant losses in CO<sub>2</sub> uptake capacities because of the reduced porosity and mass transfer and hence the accessibility of the material to CO<sub>2</sub>. It is also interesting to note that compared with the PAC0.5\_700 sample, the enhanced activation of sample PAC1.0\_700 has instead led to a sharp decrease in its volumetric adsorption capacity due to the resultant greater reduction in bulk density. This highlights the great importance of the bulk density of an adsorbent for CO<sub>2</sub> separation in practical applications.

In addition to their high CO<sub>2</sub> uptakes on both volumetric and gravimetric bases, the pitch-based AC macrospheres also possess remarkable mechanical strength, which varies from 7.51N for PAC0.5\_700 to 5.1 N for PAC1.0\_700, respectively, which are much higher than the mechanical strength of the phenolic resin-based AC beads (PR3\_700) that were found to have a maximum strength of just 2.21 N.<sup>[15a]</sup>

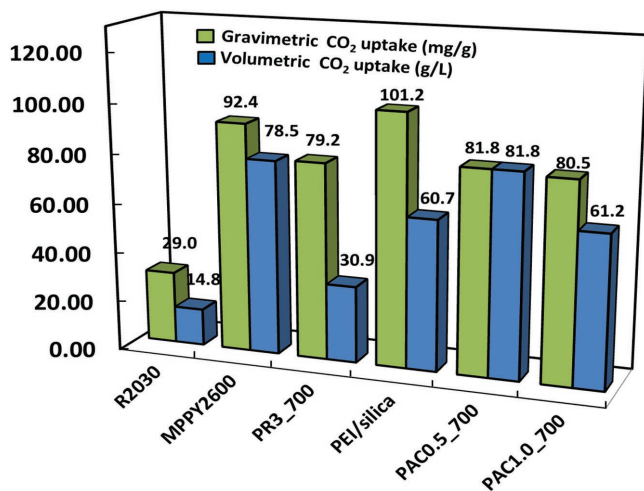


**Figure 5.** Comparison of gravimetric and volumetric CO<sub>2</sub> uptakes at 25 °C and 0.15 bar for different adsorbents (R2030: commercial carbon powder, MPPY2600: compacted carbon pellets derived from polypyrrole, PR3\_700: carbon spheres from phenolic resin, PEI/silica: with 40% PEI loading, PAC0.5\_700 and PAC1.0\_700: pitch spheres in this work, details can be found in Table 3).

### 3. Conclusion

High density and extremely ultra-microporous AC macrospheres were synthesized using coal tar pitch as the precursor via a facile sphericalization process followed by one-step mild KOH activation. The carbon macrospheres with desirable uniform diameters (1.0–2.0 mm) were found to be highly characterized by their extreme microporosities of which nearly 90% is ultra-micropores with pore diameter well below 0.8 nm.

At a CO<sub>2</sub> partial pressure of 0.15 bar, the virtually nitrogen-free AC macrospheres displayed exceedingly strong and fully reversible adsorptive properties for CO<sub>2</sub>, with uptake capacities reaching 3.2 mmol g<sup>-1</sup> at 0 °C and 1.9 mmol g<sup>-1</sup> at 25 °C. The results suggest that a combination of the high ultra-microporosity and potassium-modified surface physiochemical



properties, which can be achieved simultaneously during the preparation, is responsible for the superior adsorption performance of the carbon macrospheres.

Thanks to the very high densities achieved, the volumetric capacity of the macrospherical carbon materials, which defines the ultimate capacity that can be possibly achieved in practical terms with a capture system, reached a record of 81.2 g L<sup>-1</sup> at 25 °C and 0.15 bar, which represents the highest ever reported for both supported PEI sorbents and any other AC materials.

Coupled with the exceedingly high mechanical strength, excellent regenerability over 50 cycles, the superior performance characteristics augur very well for the sound potential of the macrospherical AC material for CO<sub>2</sub> capture in real practical applications.

#### 4. Experimental Section

**Preparation of Raw Pitch-Based Carbon Spheres:** The raw coal tar pitch with a softening temperature of 280 °C was dissolved with 30 wt% of naphthalene under stirring, following heat treatment at 150 °C for 1 h under N<sub>2</sub> atmosphere (0.5 MPa, 2 L min<sup>-1</sup>). Then the pitch was pulverized into particles of ≈0.15–1.0 mm. The blended pitch was first stirred in polyvinyl alcohol solution in an autoclave with a rotation rate of 250–300 rpm and a heating rate of 5 °C min<sup>-1</sup>. The solution was heated to 145 °C and held for 30 min. The obtained pitch spheres were washed in deionized water and dried in a vacuum oven. Sequentially, the beads were oxidized in air at 300 °C for 5 h and carbonized at 900 °C for 30 min. The parent raw pitch beads were denoted as PAC0.

**KOH Activation:** 10 g of pitch macrospheres were impregnated in KOH solution (100 mL) for 24 h. The samples were oven dried at 120 °C overnight to remove any present water. The samples were heated in horizontal tube furnace in N<sub>2</sub> at ambient pressure at 700 °C for 1 h. Then the samples were washed using deionized water until neutral. In the previous investigation (details can be found in ref. [15a]), a more effective washing method, Soxhlet extraction, was employed in order to define the correlation between the amount of residual potassium and CO<sub>2</sub> adsorption capacities. Herein, simple water washing method was applied as the experiment was designed to leave sufficient amount of intercalated potassium species according to the previous investigation. Finally, the samples were dried in the oven at 120 °C for 4 h. The resulting samples were nominated as PAC0.5\_700 and PAC1.0\_700, where 0.5 and 1.0 meant the KOH/carbon mass ratios and 700 indicated the activation temperature. Please note that for comparison, pitch spheres prepared with more KOH/carbon ratios (from 0.1 to 1.0) and activation temperatures (600, 700, and 800 °C) can be found in the Supporting Information. In addition, activated pitch carbon spheres were also developed with a multistep activation protocol (steam activation at temperatures from 600 to 850 °C, followed by KOH activation at 700 °C), and the results can be found in the Supporting Information.

**Characterization:** N<sub>2</sub> sorption isotherms were obtained at –196 °C while CO<sub>2</sub> adsorption isotherms were obtained at 0 and 25 °C, respectively, using a Micromeritics ASAP 2420 instrument. Prior to analysis, 200 mg of the samples were degassed at 150 °C for 15 h. The surface area was calculated by BET method from the N<sub>2</sub> adsorption isotherm data in the pressure range of 0.01–0.10 P/P<sub>0</sub> giving positive BET constants. Total pore volume (V<sub>total</sub>), narrow microporosity (<0.8 nm), and microporosity (<2.0 nm) pore size distributions were calculated using nonlocal density functional theory (NLDFT) carbon slit pore model, by combining the CO<sub>2</sub> adsorption isotherms at 0 °C to N<sub>2</sub> at –196 °C (beginning at 0.00005 relative pressure) using Microactive Software V3.0.

A FEI Quanta 600 SEM instrument, coupled with an energy dispersive X-ray (EDX) spectrometer (Esprit 1.9, Bruker) was applied to study the morphology of samples as well as the elemental mapping. Elemental

analysis through a LECO CHNS 628 Series was applied to detect elements N, C, H, and S. The content of K was determined by XRF on a Bruker S8 Tiger Spectrometer.

TGA (Q500, TA instruments) was also applied to test the CO<sub>2</sub> uptakes of the samples. For each test, around 25 mg of sample was first degassed at 150 °C for 45 min in N<sub>2</sub> (1 bar, 100 mL min<sup>-1</sup>), and the sample was then cooled to 25 °C. Once the temperature stabilized, flue gas containing 15% CO<sub>2</sub> in N<sub>2</sub> (1 bar, 100 mL min<sup>-1</sup>) was introduced for adsorption for 60 min. The sample was desorbed at 150 °C for 10 min. Up to 50 cycles were performed to evaluate the regeneration ability of the samples.

**Bulk Density:** Bulk density measurements were carried out using a Micromeritics AutoPore IV 9500 series MIP. An ≈0.3 g of sample was dried in a vacuum oven at 0.03 mbar at 70 °C for 24 h prior to analysis. Only low-pressure analysis was carried out for determining bulk density, with bulk density calculated at 0.0344 bar. The measurement of tap density was carried out using a Copley Tapped Density Tester Series JV1000.

**Mechanical Strength:** The mechanical strength testing of the samples was conducted using a DMA Q800 dynamic mechanical analyzer. Ten carbon beads for each sample were randomly selected for testing and the average value was reported.

#### Supporting Information

Supporting Information is available from the Wiley Online Library or from the author.

#### Acknowledgements

This work was supported by the Engineering and Physical Sciences Research Council [grant numbers EP/J020745/1, EP/G063176/1] UK; and the National Natural Science Foundation of China (Grant Nos: U1510204 and 1672291). The authors also wish to thank Dr. David Cliff from University of Nottingham for the SEM analysis.

#### Conflict of Interest

The authors declare no conflict of interest.

#### Keywords

activated carbon, CO<sub>2</sub> capture, solid adsorbent, ultra-microporous structure, volumetric CO<sub>2</sub> capacity

Received: August 16, 2017

Revised: September 24, 2017

Published online: December 18, 2017

- [1] a) M. Z. Jacobson, *Energy Environ. Sci.* **2009**, 2, 148; b) V. Scott, S. Gilfillan, N. Markusson, H. Chalmers, R. S. Haszeldine, *Nat. Clim. Change* **2013**, 3, 105.
- [2] a) A. B. Rao, E. S. Rubin, *Environ. Sci. Technol.* **2002**, 36, 4467; b) L. M. Romeo, I. Bolea, J. M. Escosa, *Appl. Therm. Eng.* **2008**, 28, 1039.
- [3] G. T. Rochelle, *Science* **2009**, 325, 1652.
- [4] a) A. Samanta, A. Zhao, G. K. Shimizu, P. Sarkar, R. Gupta, *Ind. Eng. Chem. Res.* **2011**, 51, 1438; b) S. Choi, J. H. Drese, C. W. Jones, *ChemSusChem* **2009**, 2, 796.

- [5] a) T. C. Drage, J. M. Blackman, C. Pevida, C. E. Snape, *Energy Fuels* **2009**, *23*, 2790; b) G. P. Hao, W. C. Li, D. Qian, A. H. Lu, *Adv. Mater.* **2010**, *22*, 853; c) N. Sun, Z. Tang, W. Wei, C. E. Snape, Y. Sun, *Front. Energy Res.* **2015**, *3*, 9; d) N. Sun, C. Sun, J. Liu, H. Liu, C. E. Snape, K. Li, W. Wei, Y. Sun, *RSC Adv.* **2015**, *5*, 33681.
- [6] a) D. M. D'Alessandro, B. Smit, J. R. Long, *Angew. Chem., Int. Ed.* **2010**, *49*, 6058; b) R. Wang, P. Wang, X. Yan, J. Lang, C. Peng, Q. Xue, *ACS Appl. Mater. Interfaces* **2012**, *4*, 5800; c) H. Wei, S. Deng, B. Hu, Z. Chen, B. Wang, J. Huang, G. Yu, *ChemSusChem* **2012**, *5*, 2354; d) N. P. Wickramaratne, M. Jaroniec, *J. Mater. Chem. A* **2013**, *1*, 112; e) S. Dutta, A. Bhaumik, K. C.-W. Wu, *Energy Environ. Sci.* **2014**, *7*, 3574; f) J. W. To, J. He, J. Mei, R. Haghpanah, Z. Chen, T. Kurosawa, S. Chen, W.-G. Bae, L. Pan, J. B.-H. Tok, *J. Am. Chem. Soc.* **2016**, *138*, 1001; g) H. M. Coromina, D. A. Walsh, R. Mokaya, *J. Mater. Chem. A* **2016**, *4*, 280; h) A. Arami-Niya, T. E. Rufford, Z. Zhu, *Carbon* **2016**, *103*, 115.
- [7] G.-P. Hao, W.-C. Li, D. Qian, G.-H. Wang, W.-P. Zhang, T. Zhang, A.-Q. Wang, F. Schüth, H.-J. Bongard, A.-H. Lu, *J. Am. Chem. Soc.* **2011**, *133*, 11378.
- [8] J. Wang, L. Huang, R. Yang, Z. Zhang, J. Wu, Y. Gao, Q. Wang, D. O'Hare, Z. Zhong, *Energy Environ. Sci.* **2014**, *7*, 3478.
- [9] a) J. P. Marco-Lozar, M. Kunowsky, F. Suárez-García, A. Linares-Solano, *Carbon* **2014**, *72*, 125; b) J. Wang, A. Heerwig, M. R. Lohe, M. Oschatz, L. Borchardt, S. Kaskel, *J. Mater. Chem.* **2012**, *22*, 13911.
- [10] a) A. Arenillas, K. Smith, T. Drage, C. Snape, *Fuel* **2005**, *84*, 2204; b) T. C. Drage, A. Arenillas, K. M. Smith, C. Pevida, S. Piippo, C. E. Snape, *Fuel* **2007**, *86*, 22; c) M. Plaza, C. Pevida, A. Arenillas, F. Rubiera, J. Pis, *Fuel* **2007**, *86*, 2204; d) B. Zhu, K. Li, J. Liu, H. Liu, C. Sun, C. E. Snape, Z. Guo, *J. Mater. Chem. A* **2014**, *2*, 5481; e) M. Sevilla, P. Valle-Vigón, A. B. Fuertes, *Adv. Funct. Mater.* **2011**, *21*, 2781; f) Y. Li, B. Zou, C. Hu, M. Cao, *Carbon* **2016**, *99*, 79.
- [11] L. Wan, J. Wang, C. Feng, Y. Sun, K. Li, *Nanoscale* **2015**, *7*, 6534.
- [12] a) T. Kyotani, T. Nagai, S. Inoue, A. Tomita, *Chem. Mater.* **1997**, *9*, 609; b) J. Marco-Lozar, J. Juan-Juan, F. Suárez-García, D. Cazorla-Amorós, A. Linares-Solano, *Int. J. Hydrogen Energy* **2012**, *37*, 2370; c) J. Marco-Lozar, M. Kunowsky, F. Suárez-García, J. Carruthers, A. Linares-Solano, *Energy Environ. Sci.* **2012**, *5*, 9833.
- [13] a) T. Otowa, Y. Nojima, T. Miyazaki, *Carbon* **1997**, *35*, 1315; b) J. Wang, S. Kaskel, *J. Mater. Chem.* **2012**, *22*, 23710.
- [14] B. Viswanathan, P. Indra Neel, T. Varadarajan, India, Chennai 600 036 **2009**, 1.
- [15] a) J. Liu, N. Sun, C. Sun, H. Liu, C. Snape, K. Li, W. Wei, Y. Sun, *Carbon* **2015**, *94*, 243; b) X. Liu, Y. Sun, J. Liu, C. Sun, H. Liu, Q. Xue, E. Smith, C. Snape, *ACS Applied Materials & Interfaces* **2017**, *9*, 26826.
- [16] a) Y. Zou, M. Park, S. Hong, M. S. Lah, *Chem. Commun.* **2008**, 2340; b) H. Wu, R. S. Reali, D. A. Smith, M. C. Trachtenberg, J. Li, *Chem. - Eur. J.* **2010**, *16*, 13951; c) B. Zheng, J. Bai, J. Duan, L. Wojtas, M. J. Zaworotko, *J. Am. Chem. Soc.* **2010**, *133*, 748; d) A. Wahby, J. M. Ramos-Fernández, M. Martínez-Escandell, A. Sepúlveda-Escribano, J. Silvestre-Albero, F. Rodríguez-Reinoso, *ChemSusChem* **2010**, *3*, 974.
- [17] E. Raymundo-Pinero, P. Azais, T. Cacciaguerra, D. Cazorla-Amorós, A. Linares-Solano, F. Béguin, *Carbon* **2005**, *43*, 786.
- [18] V. Presser, J. McDonough, S.-H. Yeon, Y. Gogotsi, *Energy Environ. Sci.* **2011**, *4*, 3059.
- [19] Z. Zhang, J. Zhou, W. Xing, Q. Xue, Z. Yan, S. Zhuo, S. Z. Qiao, *Phys. Chem. Chem. Phys.* **2013**, *15*, 2523.
- [20] a) A. S. Jalilov, Y. Li, J. Tian, J. M. Tour, *Adv. Energy Mater.* **2017**, *7*, 1600693; b) G. Srinivas, V. Krungleviciute, Z.-X. Guo, T. Yildirim, *Energy Environ. Sci.* **2014**, *7*, 335; c) G. Singh, I. Y. Kim, K. S. Lakhi, P. Srivastava, R. Naidu, A. Vinu, *Carbon* **2017**, *116*, 448.
- [21] a) A. Phan, C. J. Doonan, F. J. Uribe-Romo, C. B. Knobler, M. O'keeffe, O. M. Yaghi, *Acc. Chem. Res.* **2010**, *43*, 58; b) J.-R. Li, Y. Ma, M. C. McCarthy, J. Sculley, J. Yu, H.-K. Jeong, P. B. Balbuena, H.-C. Zhou, *Coord. Chem. Rev.* **2011**, *255*, 1791; c) Y. Zhao, X. Liu, K. X. Yao, L. Zhao, Y. Han, *Chem. Mater.* **2012**, *24*, 4725.
- [22] a) G. Pirngruber, P. Raybaud, Y. Belmabkhout, J. Čejka, A. Zukal, *Phys. Chem. Chem. Phys.* **2010**, *12*, 13534; b) A. Pulido, P. Nachtigall, A. Zukal, I. Domínguez, J. i. Čejka, *J. Phys. Chem. C* **2009**, *113*, 2928.
- [23] Y. Xia, R. Mokaya, G. S. Walker, Y. Zhu, *Adv. Energy Mater.* **2011**, *1*, 678.
- [24] S.-M. Hong, S. W. Choi, S. H. Kim, K. B. Lee, *Carbon* **2016**, *99*, 354.
- [25] R. Chahine, T. Bose, *Int. J. Hydrogen Energy* **1994**, *19*, 161.
- [26] W. Zhang, H. Liu, Y. Sun, J. Cakstins, C. Sun, C. E. Snape, *Appl. Energy* **2016**, *168*, 394.
- [27] B. Adeniran, R. Mokaya, *Nano Energy* **2015**, *16*, 173.
- [28] R. T. Woodward, L. A. Stevens, R. Dawson, M. Vijayaraghavan, T. Hasell, I. P. Silverwood, A. V. Ewing, T. Ratvijitvech, J. D. Exley, S. Y. Chong, *J. Am. Chem. Soc.* **2014**, *136*, 9028.
- [29] X. Ma, Y. Li, M. Cao, C. Hu, *J. Mater. Chem. A* **2014**, *2*, 4819.